AD-754 212

STUDY OF NUMERICAL METHODS IN SEISMIC PROBLEMS

D. W. McCowan, et al

Teledyne Geotech

Prepared for:

Advanced Research Projects Agency
Air Force Office of Scientific Research

7 September 1972

DISTRIBUTED BY:

NTIS

National Technical Information Service
U. S. DEPARTMENT OF COMMERCE
5285 Port Royal Road, Springfield Va. 22151

BEST
AVAILABLE COPY

AFOSR - TR - 73 - 0011

AL-72-2

AD754212

.....contributing to man's understanding of the environment world

STUDY OF NUMERICAL METHODS IN SEISMIC PROBLEMS

BY

D.W. McCOWAN, C.A. NEWTON, E.A. PAGE, A.F. PETERSON and E.A. FLINN

SPONSORED BY
ADVANCED RESEARCH PROJECTS AGENCY

MONITORED BY
AIR FORCE OFFICE OF SCIENTIFIC RESEARCH

ARPA ORDER NO. 1357

7 SEPTEMBER 1972

D D C
RECEIVED
JAN 26 1973
B

TELEDYNE GEOTECH
ALEXANDRIA LABORATORIES

Reproduced by
NATIONAL TECHNICAL
INFORMATION SERVICE
U S Department of Commerce
Springfield VA 22151

Approved for public release;
distribution unlimited.

61

Unclassified

Security Classification

DOCUMENT CONTROL DATA - R&D

(Security classification of title, body of abstract and indexing annotation must be entered when the overall report is classified)

1. ORIGINATING ACTIVITY (Corporate author)
Teledyne Geotech
Alexandria, Virginia

2a. REPORT SECURITY CLASSIFICATION
Unclassified

2b. GROUP

3. REPORT TITLE
STUDY OF NUMERICAL METHODS IN SEISMIC PROBLEMS

4. DESCRIPTIVE NOTES (Type of report and inclusive dates)
Scientific .....INTERIM

5. AUTHOR(S) (Last name, first name, initial)
McCowan, D.W.; Newton, C.A.; Page, E.A.; Peterson, A.F.; and Flinn, E.A.

6. REPORT DATE
7 September 1972

7a. TOTAL NO. OF PAGES
~~58~~ 61

7b. NO. OF REFS
12

8a. CONTRACT OR GRANT NO.
F44620-69-C-0082

b. PROJECT NO.
AO 1357

c.
62701D

d.

8b. ORIGINATOR'S REPORT NUMBER(S)
AL-72-2

9b. OTHER REPORT NO(S) (Any other numbers that may be assigned this report)
AFOSR - TR - 73 - 0011

10. AVAILABILITY/LIMITATION NOTICES
Approved for public release; distribution unlimited.

11. SUPPLEMENTARY NOTES
TECH OTHER

12. SPONSORING MILITARY ACTIVITY
Air Force Office of Scientific Res.
1400 Wilson Boulevard NPG
Arlington, Virginia

13. ABSTRACT
We have investigated the application of two numerical methods (finite element and finite difference approximations) toward the ultimate solution of problems involving the propagation of Rayleigh waves generated by an explosion in the atmosphere over an island atoll. Because of mathematical difficulties in these methods, which we discuss in detail, we were unable to obtain useful calculations of Rayleigh wave spectra at teleseismic distances. It appears that the physical constraints of the atoll structure, e.g., abrupt changes in elastic properties in both lateral and vertical directions, require either the application of large and costly computer codes or an advance in the present state of the art in numerical simulation. We offer examples of numerical solutions to problems which have known analytic solutions. Further study of these problems is being continued at The Pennsylvania State University under another project.

14. KEY WORDS
Finite difference calculations
Finite element calculations
Rayleigh waves
Atmospheric nuclear explosions
Seismic wave excitation

Unclassified

Security Classification

STUDY OF NUMERICAL METHODS
IN SEISMIC PROBLEMS

ALEXANDRIA LABORATORIES REPORT NO. AL-72-2

Effective Date of Contract:	1 March 1969
Contract Expiration Date:	31 March 1972
Amount of Contract Dollars:	$ 590,572
Program Code:	1F10
Contract Number:	F44620-69-C-0082
ARPA Order No.:	1357
Principal Investigator:	Carl A. Newton
Period Covered:	1 March 1969 through 31 March 1972

Approved for public release;
distribution unlimited.

TABLE OF CONTENTS

	Page No.
ABSTRACT	
INTRODUCTION	1
FINITE DIFFERENCE APPROACH	6
Stability condition	13
Method for handling velocity changes without specifying boundary conditions	18
Free surface	21
Non-reflecting boundary	24
FINITE ELEMENT METHOD	27
REFERENCES	38
ACKNOWLEDGEMENTS	40

LIST OF FIGURES

Figure Title	Figure No.
Schematic diagram of the finite difference displacement calculation.	1
Representation of the derivatives of the elastic parameters at material boundaries for the finite difference method.	2
Transmission and reflection of a pulse at a material boundary using the finite difference method.	3
Material mesh which gives satisfactory difference equations at the free surface.	4
Longitudinal displacement of the "standard" one-dimensional rod with square wave pulse input.	5
Longitudinal displacement of the "standard" one-dimensional rod with Gaussian shaped pulse input.	6
"Snapshots" of longitudinal displacements in a rod where the elements double in length following nodes 19 and 20, at times between 0.0019 and 0.0059 seconds.	7
Homogeneous isotropic halfspace mesh used for solving Lamb's problem.	8
u displacement for Lamb's problem with unconstrained surface stress.	9
w displacement for Lamb's problem with unconstrained surface stress.	10
f-k plot of w component for Lamb's problem with unconstrained surface stress. Contour interval is 3 db.	11

LIST OF FIGURES (Cont'd.)

Figure Title	Figure No.
u displacement for Lamb's problem with constrained surface stress.	11a
w displacement for Lamb's problem with constrained surface stress.	11b
f-k plot of w component for Lamb's problem with constrained surface stress.	12
Displacement of the node point at the origin of the mesh shown in Figure 8.	13

INTRODUCTION

The objective of the research described in this report was to predict the spectrum of Rayleigh waves generated by a nuclear explosion over an island atoll, as recorded at teleseismic distances. Our approach was a computational one, since this problem cannot at present be handled theoretically: generation of the seismic waves takes place within a small distance of ground zero (which is assumed to be located near the middle of the atoll), and this implies that the coupling of energy from the explosion-generated shock wave in the atmosphere into seismic waves in the earth is characteristic of the shallow water depth typical of the interior of atolls of the type we are considering. On the other hand, a major influence in shaping the spectrum of teleseismic Rayleigh waves is the deep ocean structure which surrounds the island, through which the Rayleigh waves propagate most of the way to the recording stations. The transition from shallow to deep water takes place well within the critical distance for Rayleigh wave generation, so even the approximate coupling techniques developed by McGarr and Alsop (1967) and McGarr (1969) are inapplicable. The basic difficulty is that at the present time theory cannot handle laterally inhomogeneous structures with the necessary precision, and it is obviously wrong to assume a laterally homogeneous oceanic structure between the island source and the continental station.

Consequently, we thought of applying numerical techniques to carry the shock wave from the atmosphere

through the shallow water and the island structure into the deep ocean: the distributions of elastic displacements and stresses with depth completely specify the input to a well-known problem which has a unique solutuion, viz., Rayleigh wave propagation in a laterally homogeneous horizontally plane-layered medium.

Since the seismic stations are located on continents, we anticipated being able to use McGarr's theory for predicting what happens at the continental margin. An alternative, once programs for numerical calculations of elastic wave propagation in an inhomogeneous media were developed, would be to model numerically the Rayleigh wave propagation through the ocean/continent boundary.

We anticipated that this would be a fairly straightforward project. Delineation of the problem is easy, material properties of the type of structure in question are known, it is quite simple to set out a procedure for attacking the problem, and after all, numerical calculation of elastic wave propagation in solids has been intensively studied for years; for example by Holzer and his colleagues (1966), and by Alterman and her colleagues (Alterman et al., 1970).

We were wrong, in that it now appears that the problem is beyond the state of the art of numerical analysis, and our project ended before we were able to advance that particular frontier sufficiently to solve the atoll problem.

We started with the most elementary approach: an explicit finite difference scheme (in both time and

space) in which the derivatives in the wave equation were approximated by finite difference expressions. As a starting point we used the program described by Alterman in a number of papers, which Professor Alterman generously made available to us, but it soon became clear that that program could not easily be converted to the cylindrical symmetry we required.

We therefore programmed a finite difference code in which cylindrical symmetry was built in. The inhomogeneous elastic wave equation is rather complicated, and for checking out the analysis we found it very useful to have access to a FORMAC program, (Tobey, 1967). This list processing system was able to take in the multi-dimensional tensor equations and produce the final difference approximation in FORTRAN language, with which we could compare and verify our own deviation and programming.

It is prudent to approach computers with the same apprehension and care that bullfighters use in their work, so we started with simple test cases whose solutions are known analytically. It soon became apparent that there are inherent difficulties in the finite difference method, namely:

1. The inhomogeneities of material properties in the problem are abrupt: air to water, water to rock, crust to mantle; in addition, these material inhomogeneities are two-dimensional (i.e., r and z variation) and also the source function is discontinuous in time. These factors appear to cause unavoidable instabilities in the numerical calculations.

2. The source function is applied to one of the boundaries on which material properties are discontinuous. This also appears to cause instability.

3. Even though we used a high-speed computer with ten tape units, 32K words of core, and a large disc, it was very difficult to arrange to make the mesh large enough to avoid spurious reflections from the artificial boundaries caused by terminating the mesh: the P waves went out and back before the Rayleigh waves ever got to the deep ocean.

C. Constantino and F.C. Karal discussed these questions with us at length (private communication, 1970). The concensus was that the difficulties are indeed inherent in finite difference approximations to dymanic problems. We subsequently found that even an implicit scheme, rather than an explicit one, did not solve these difficulties.

We therefore decided to use a finite element scheme rather than a finite difference scheme. The finite element method has been used for many years in static problems of structural mechanics. In this method the material is divided into small homogeneous polygonal elements which are welded together along their edges. The elastic wave equation is solved analytically in each individual element under the single assumption that the displacement varies linearly along the edges of the elements. Basically, the method works because the displacements at the vertices of each element, as calculated in each of the contiguous elements, must all be the same. This fact leads to condition equations

which are easily solved if a large enough computer is available.

Unfortunately, even after very considerable effort we were unable to produce correct answers for elementary problems in which shock waves are applied to a material discontinuity. A detailed discussion is given in the following sections. Further work on this problem is currently a part of a Ph.D. program in the Department of Geophysics at the Pennsylvania State University.

FINITE DIFFERENCE APPROACH

The finite difference approximation to numerical solution of elastodynamic problems is well known; see, for example, references given by Alterman et al. (1970). In this approach the derivatives of the wave function with respect to time, and the spatial derivatives of the material properties, are approximated by finite differences.

In this section we discuss our development of this approach in some detail.

The elastic wave equation is:

$$(\lambda + \mu)\, \overline{\nabla}\, (\overline{\nabla}\cdot\overline{S}) + (\overline{\nabla}\cdot\overline{S})(\overline{\nabla}\lambda) + \mu\, \overline{\nabla}^2 \overline{S}$$

$$+ \left[(\overline{\nabla}\mu\cdot\overline{\nabla})\overline{S} + \overline{\nabla}(\overline{\nabla}\mu\cdot\overline{S})\right] = \rho_o \ddot{\overline{S}}$$

Here the displacement $\overline{S} = \overline{S}\,(u,v,w)$ and λ, μ and ρ_o, the elastic constants and density respectively, are functions of position. Neglecting second derivatives of the elastic constants one obtains the following for the u component equation in rectangular coordinates:

$$\rho_o \ddot{u} = (\lambda + \mu)\left[\frac{\partial^2 u}{\partial x^2} + \frac{\partial^2 v}{\partial x \partial y} + \frac{\partial^2 w}{\partial x \partial z}\right]$$

$$+ \mu\left[\frac{\partial^2 u}{\partial x^2} + \frac{\partial^2 u}{\partial y^2} + \frac{\partial^2 u}{\partial z^2}\right] + \frac{\partial u}{\partial x}\left(\frac{\partial x}{\partial x} + 2\frac{\partial \mu}{\partial x}\right) \tag{1}$$

$$+ \frac{\partial x}{\partial x}\left(\frac{\partial v}{\partial y} + \frac{\partial w}{\partial z}\right) + \frac{\partial \mu}{\partial y}\left(\frac{\partial u}{\partial y} + \frac{\partial v}{\partial x}\right)$$

$$+ \frac{\partial \mu}{\partial z}\left(\frac{\partial u}{\partial z} + \frac{\partial w}{\partial x}\right)$$

where $\lambda = \lambda(x,y,z)$, $\mu = \mu(x,y,z)$, $\rho_o = \rho_o(x,y,z)$ and the displacement in the $\bar{e}_x$ direction. The equations of motion for the v and w displacement component, ($\bar{e}_y$ and $\bar{e}_z$ directions), have the same form as equation (1).

These equations in cylindrical coordinates are:

$$\rho_o \ddot{u} = (\lambda+2\mu)\left[\frac{\partial^2 u}{\partial r^2} + \frac{\partial^2 w}{\partial r \partial z} - \frac{u}{r^2} - \frac{\partial v}{\partial \phi}\frac{1}{r^2} + \frac{\partial u}{\partial r}\frac{1}{r}\right.$$

$$\left. + \frac{\partial^2 v}{\partial r \partial \phi}\frac{1}{r}\right] + \mu\left[\frac{\partial^2 u}{\partial z^2} + \frac{\partial^2 u}{\partial \phi^2}\frac{1}{r^2} - \frac{\partial^2 w}{\partial r \partial z}\right.$$

$$\left. - \frac{\partial^2 v}{\partial r \partial \phi}\frac{1}{r} - \frac{\partial v}{\partial \phi}\frac{1}{r^2}\right] + \frac{\partial u}{\partial r}\left(2\frac{\partial \mu}{\partial r}\right) + \frac{\partial \mu}{\partial \phi}\left(\frac{1}{r^2}\frac{\partial u}{\partial \phi}\right.$$

$$\left. + \frac{1}{r}\frac{\partial v}{\partial r} - \frac{v}{r^2}\right) + \frac{\partial u}{\partial z}\left(\frac{\partial u}{\partial z} + \frac{\partial w}{\partial r}\right) + \frac{\partial \lambda}{\partial r}\left(\frac{u}{r}\right.$$

$$\left. + \frac{1}{r}\frac{\partial v}{\partial \phi} + \frac{\partial w}{\partial z} + \frac{\partial u}{\partial r}\right)$$

$$\rho_o \ddot{v} = (\lambda+2\mu)\left[\frac{\partial u}{\partial \phi}\frac{1}{r^2} + \frac{\partial^2 v}{\partial \phi^2}\frac{1}{r^2} + \frac{\partial^2 u}{\partial r \partial \phi}\frac{1}{r} + \frac{\partial^2 w}{\partial \phi \partial z}\frac{1}{r}\right]$$

$$+ \mu\left[\frac{\partial^2 v}{\partial r^2} + \frac{\partial^2 v}{\partial z^2} - \frac{\partial^2 u}{\partial r \partial \phi}\frac{1}{r} - \frac{\partial^2 w}{\partial \phi \partial z} + \frac{\partial u}{\partial \phi}\frac{1}{r^2} + \frac{\partial v}{\partial r}\frac{1}{r} - \frac{v}{r^2}\right]$$

$$+ \frac{\partial \lambda}{\partial \phi}\left[\frac{u}{r^2} + \frac{\partial v}{\partial \phi}\frac{1}{r^2} + \frac{\partial u}{\partial r}\frac{1}{r^2} + \frac{\partial u}{\partial r}\frac{1}{r} + \frac{\partial w}{\partial z}\frac{1}{r}\right] + 2\frac{\partial u}{\partial \phi}\left(\frac{u}{r^2} + \frac{\partial v}{\partial \phi}\frac{1}{r^2}\right)$$

$$+ \frac{\partial \mu}{\partial r}\left[\frac{\partial v}{\partial r} - \frac{v}{r} + \frac{\partial u}{\partial \phi}\frac{1}{r}\right] + \frac{\partial u}{\partial z}\left(\frac{\partial w}{\partial \phi}\frac{1}{r} + \frac{\partial v}{\partial z}\right)$$

$$\rho_o \ddot{w} = (\lambda+2\mu)\left[\frac{\partial^2 u}{\partial r \partial z} + \frac{1}{r}\frac{\partial u}{\partial z} + \frac{\partial^2 v}{\partial \phi \partial z}\frac{1}{r} + \frac{\partial^2 w}{\partial z^2}\right]$$

$$+ \mu\left[\frac{\partial^2 w}{\partial r^2} + \frac{\partial^2 w}{\partial \phi^2}\frac{1}{r^2} + \frac{\partial w}{\partial r}\frac{1}{r} - \frac{\partial^2 u}{\partial r \partial z} - \frac{\partial u}{\partial z}\frac{1}{r} - \frac{\partial^2 v}{\partial \phi \partial z}\frac{1}{r}\right]$$

$$+ \frac{\partial \lambda}{\partial z}\left[\frac{u}{r} + \frac{1}{r}\frac{\partial v}{\partial \phi} + \frac{\partial u}{\partial r} + \frac{\partial w}{\partial z}\right] + \frac{\partial \mu}{\partial \phi}\left(\frac{\partial w}{\partial \phi}\frac{1}{r^2} + \frac{\partial v}{\partial z}\frac{1}{r}\right)$$

$$+ \frac{\partial u}{\partial r}\left(\frac{\partial u}{\partial z} + \frac{\partial w}{\partial r}\right) + \frac{\partial \mu}{\partial z}\left(2\frac{\partial w}{\partial z}\right)$$

where $\lambda = \lambda(r,\phi,z)$, $\mu = \mu(r,\phi,z)$, $\rho_o = \rho_o(r,\phi,z)$ and u,v and w are the displacements in the $\bar{e}_r$, $\bar{e}_\theta$ and $\bar{e}_z$ directions respectively.

The cases we are presently interested in are those having axial symmetry, in which case the equations reduce to:

$$\rho_o \ddot{u} = (\lambda+2\mu)\left[\frac{\partial^2 u}{\partial r^2} + \frac{\partial^2 w}{\partial r \partial z} - \frac{u}{r^2} + \frac{\partial u}{\partial r}\frac{1}{r}\right]$$

$$+ \mu\left[\frac{\partial^2 u}{\partial z^2} - \frac{\partial^2 w}{\partial r \partial z}\right] + \frac{\partial u}{\partial r}\left(2\frac{\partial \mu}{\partial r}\right) + \frac{\partial \mu}{\partial z}\left(\frac{\partial u}{\partial z} + \frac{\partial w}{\partial r}\right) \qquad (2a)$$

$$+ \frac{\partial \lambda}{\partial r}\left(\frac{u}{r} + \frac{\partial w}{\partial z} + \frac{\partial u}{\partial r}\right)$$

$$\rho_o \ddot{v} = \mu\left[\frac{\partial^2 v}{\partial r^2} + \frac{\partial^2 v}{\partial z^2} + \frac{\partial v}{\partial r}\frac{1}{r} - \frac{v}{r^2}\right] + \frac{\partial \mu}{\partial r}\left(\frac{\partial v}{\partial r} - \frac{v}{r}\right) + \frac{\partial \mu}{\partial z}\frac{\partial v}{\partial z}$$

$$\rho_o \ddot{w} = (\lambda+2\mu\ [\frac{\partial^2 u}{\partial r \partial z} + \frac{1}{r}\frac{\partial u}{\partial z} + \frac{\partial^2 w}{\partial z^2}] + \mu[\frac{\partial^2 w}{\partial r^2}$$

$$+ \frac{1}{r}\frac{\partial w}{\partial r} - \frac{\partial^2 u}{\partial r \partial z} - \frac{\partial u}{\partial z}\frac{1}{r}] + \frac{\partial \lambda}{\partial z}[\frac{u}{r} + \frac{\partial u}{\partial r} + \frac{\partial w}{\partial z}] \qquad (2b)$$

$$+ \frac{\partial \mu}{\partial r}(\frac{\partial u}{\partial z} + \frac{\partial w}{\partial r}) + \frac{\partial \mu}{\partial z}\ 2\frac{\partial w}{\partial z}$$

We notice that the displacements in the $\bar{e}_r$ and $\bar{e}_z$ directions are completely uncoupled to displacements in the $\bar{e}_\theta$ direction.

For an explicit finite difference solution of these equations one approximates the derivatives by either backward, centered, or forward differences (except for the derivatives of the elastic constants, which will be discussed later). In regions other than the free surface (to be discussed later) it is generally accepted that centered differences usually give the most accurate results.

Thus, with $r = m\Delta r$, $z = n\Delta z$ and $t = \rho\Delta t$, where m,n, and p are integers, the derivative approximation would be of the form:

$$\frac{\partial u(r,z,t)}{\partial t} \approx \frac{u_{m,n,p+1} - 2u_{m,n,p} + u_{m,n,p-1}}{(\Delta t)^2}$$

$$\frac{\partial^2 u(r,z,t)}{\partial r \partial z} \approx$$

$$\frac{u_{m+1,n+1,p} + u_{m-1,\ n-1,p} - u_{m-1\ n+1,p} - u_{m+1,n-1,p}}{4(\Delta r)(\Delta z)}$$

Substitutions into equations (2) leads to an explicit solution of the form:

$$\begin{aligned} u_{m,n,p+1} = & -u_{m,n,p-1} + au_{m,n,p} + bu_{m+1,n,p} \\ & + b'u_{m-1,n,p} + cu_{m,n+1,p} + c'u_{m,n-1,p} \\ & + d(w_{m+1,m,p} - w_{m-1,n,p}) \\ & + e(w_{m,n+1,p} - w_{m,n-1,p}) \\ & + f(w_{m+1,n+1,p} + w_{m-1,n-1,p} - w_{m+1,n-1,p} \\ & - w_{m-1,n-1,p}) \end{aligned}$$

and a similar form for the w component. Thus, knowledge of displacements at times $p\Delta t$ and $(p-1)\Delta t$ in a neighborhood of locations about the point (m,n) enables one to calculate displacements at time $(p+1)\Delta t$.

Stability condition

The selection of increments Δr, Δz, and Δt is not arbitrary, since the difference equations must satisfy a stability condition, which the case of the wave equation insures that information does not flow faster in the finite difference scheme than it does in the medium being modelled. Stability conditions can be derived for the given form of the wave equation using a number of different methods, all of which involve a great deal of calculation and ultimately only give approximate stability conditions. We use instead a new method which gives the exact stability condition quite easily for the elastic wave equation: setting the coefficients of the u(m,n,p) term equal to zero yields, in the appropriate limits, the approximate stability conditions obtained by the other methods.

For the axisymmetric case the approximate stability condition is:

$$\Delta t \leq \left(\frac{\Delta r}{\alpha}\right)\left[1+\left(\frac{\beta}{\alpha}\right)^2\right]^{-1/2}$$

where

$$\alpha = \left(\sqrt{\frac{\lambda+2\mu}{\rho_o}}\right)^{1/2}$$

and

$$\beta = \left(\sqrt{\frac{\mu}{\rho_o}}\right)^{1/2}$$

If we look at the finite difference expression for the u component, where

$$u_{m,n,p+1} = -u_{m,n,p-1} + 2u_{m,n,p}[1-A(1 + \frac{1}{2(m-1)^2})$$

$$- B+ \frac{\lambda_r(\Delta t)^2}{2(m-1)\rho_o\Delta r}] + u_{m+1,n,p}[A(1 + \frac{1}{2(m-1)} + \frac{\mu_r(\Delta t)^2}{\rho_o\Delta r}$$

$$+ \frac{\lambda_r}{2\rho_o}(\frac{\Delta t}{\Delta r})^2] + u_{m,n+1,p}(B + \frac{\mu_z(\Delta t)^2}{2\rho_o\Delta r})$$

$$+ u_{m,n-1,p}(B - \frac{\mu_z(\Delta t)^2}{2\rho_o\Delta t})$$

$$+ \left(w_{m+1,n,p} - w_{m-1,n,p}\right) \frac{\mu_z (\Delta t)^2}{2\rho_o \Delta r}$$

$$+ \left(W_{m,n+1,p} - w_{m,n-1,p}\right) \frac{\lambda_r (\Delta t)^2}{2\rho_o (\Delta z)}$$

$$+ .25(A+8)\left(w_{m+1,n+1,p} + w_{m-1,n-1,p} - w_{m+1,n-1,p}\right.$$

$$\left. - w_{m-1,n+1,p}\right)$$

where

$$\lambda_r = \frac{\partial \lambda}{\partial r} \; ; \qquad A = \frac{(\lambda + 2\mu)}{\rho_o} \left(\frac{\Delta t}{\Delta r}\right)^2 \; ; \qquad B = \frac{\mu}{\rho_o} \left(\frac{\Delta t}{\Delta r}\right)^2$$

$$\mu_r = \frac{\partial \mu}{\partial r} \; ; \qquad \mu_z = \frac{\partial \mu}{\partial z}$$

We see that setting the coefficient of the u(m,n,p) term equal to zero yields the stability condition:

$$\Delta t \leq \left[\left(\frac{\alpha}{\Delta r}\right)^2 \left(1 + \frac{1}{2(m-1)^2}\right) + \left(\frac{\alpha}{\Delta z}\right)^2 - \frac{\lambda_r}{2(m-1)\rho_o \Delta r}\right]^{-1/2}$$

which reduces to the earlier expression when $\Delta Z = \Delta r$ and $m \to \infty$.

For the w component of displacement one has a different stability condition. The finite difference expression for the w component is:

$$w_{m,n,p+1} = -w_{m,n,p-1} + -w_{m,n,p}\left(1 - A - B + \frac{\lambda_2(\Delta t)^2}{2\rho_o(m-1)\Delta r}\right) + w_{m,n+1,p}\left(A + \frac{\lambda_z(\Delta t)^2}{2\rho_o \Delta z} + \frac{\mu_z(\Delta t)^2}{\rho_o \Delta z}\right.$$

$$+ w_{m,n-1,p}\left(A - \frac{\lambda_z(\Delta t)^2}{2\rho_o \Delta z} - \frac{\mu_z(\Delta t)^2}{\rho_o \Delta z}\right.$$

$$+ w_{m+1,n,p}\left[B\left(1 + \frac{1}{2(m-1)} - \frac{\mu_r(\Delta t)^2}{2\rho_o \Delta r}\right]\right.$$

$$+ (u_{m,n+1,p} - u_{m,n-1,p}) \left(\frac{A}{2(m-1)} - \frac{B}{2(m-1)}\right.$$

$$+ .25 (A+B) (u_{m+1,n+1,p} + u_{m-1,n-1,p}$$

$$- u_{m+1,n-1,p} - u_{m-1,n+1,p})$$

$$\Delta t \leq \left[\left(\frac{\alpha}{\Delta z}\right)^2 + \left(\frac{\beta}{\Delta r}\right)^2 - \frac{\lambda_z}{2\rho_o(m-1)\Delta r}\right]^{-1/2}$$

which gives for the stability condition

$$\Delta t \leq \left[\left(\frac{\alpha}{\Delta z}\right)^2 + \left(\frac{\beta}{\Delta r}\right)^2 - \frac{\lambda_z}{2\rho_o(m-1)\Delta r}\right]^{-1/2}$$

These relations were checked by running sample cases, and the additional terms included found to be valid, i.e., they do set the limit on the point at which instabilities develop. Changes in the elastic constants enter these expressions, and we see that knowing the exact stability condition is very important when dealing with abrupt velocity changes, since at certain boundaries or corners non-stable effects may develop and gradually contaminate the rest of the problem.

Method for handling velocity changes without specifying boundary conditions

If one uses the homogeneous form of the elastic wave equation to solve a problem in which there are several velocity discontinuities, solutions are obtained by matching boundary conditions for each point at which there is a velocity change. This approach is impractical for complicated velocity distributions. If one uses the heterogeneous elastic wave equation (as we do in this report) the elastic parameters and their space derivatives are input and the boundary conditions are automatically satisfied within the equation.

One might expect that the spatial derivative of λ and μ could be handled in the same manner as for the derivatives of displacement (using central differences); however, this method gives incorrect results. A method which does work involves spreading velocity changes over two grid points with the boundary point having a

velocity $(v_1 + v_2)/2$, where v_1 and v_2 are the velocities of the adjoining velocity zones. One then takes the derivatives of the elastic parameters λ and μ to be zero at the mesh points before and after the boundary point and approximates the derivative at the boundary by a centered difference. This procedure is illustrated in Figures 2 for the case $\mu = 0$.

If this procedure is used while holding the stability factor and time increment Δt constant (or the stability factor and Δr or Δz, according to the direction of the velocity change), excellent transmission and reflection amplitudes are obtained. Transmission and reflection results are shown in Figure 3 for the problem in which the P velocity varies in one dimension from 1 to 2, and $\mu = 0$. In general both shear and longitudinal waves are present. One now needs to pick λ and μ values at the boundary such that both the longitudinal and shear velocities make a linear transition from one medium to the other. We first pick μ_B, the value of μ at the boundary, to be

$$\mu_B = \frac{1}{4} \left(\sqrt{\mu_1} + \sqrt{\mu_2}\right)^2$$

(assuming ρ_o to be unchanged), thus setting the shear velocity at the boundary. Then one can set the longitudinal velocity at the boundary by setting the value of λ at the boundary:

$$\lambda_B = \frac{1}{4}\left(\sqrt{\lambda_1+2\mu_1} + \sqrt{\lambda_2+2\mu_2}\right)^2 - 2\mu_B$$

This can be extended to the case where ρ, λ, and μ all change at the boundary. First we pick a linear change in ρ:

$$\rho_B = \frac{\rho_1+\rho_2}{2}$$

Then we pick a linear β change

$$\mu_B = \frac{1}{4}\left(\frac{\mu_1}{\rho_1} + \frac{\mu_2}{\rho_2}\right)^2 \rho_B$$

Thus we can satisfy the condition

$$\lambda_B = \frac{1}{4}\left(\frac{\lambda_1+2\mu_1}{\rho_1} + \frac{\lambda_2+2\mu_2}{\rho_2}\right)^2 \rho_B - 2\mu_B$$

Thus one-dimensional velocity changes in a medium can be handled by:

a) spreading velocity changes over two mesh points,

b) picking values of ρ,λ and μ at the boundary point such that the velocities make linear transitions, and

c) setting the derivative of the elastic parameters equal to zero except at the boundary point and using a central difference there.

This method is very effective for cases in which

there is inhomogeneity in only one direction, but unfortunately cannot be extended to cases with two- or three-dimensional velocity variations (private communication, C. Costantino).

Free surface

Accounting for the free surface is another aspect of the problem in which the centered difference approximation is not satisfactory. Consider the mesh defined in Figure 4.

To take the derivatives

$$\left.\frac{\partial u(r,z,t)}{\partial z}\right|_{z=0}$$

and

$$\left.\frac{\partial u(r,z,t)}{\partial r}\right|_{z=0}$$

one would expect to be able to write

$$\left.\frac{\partial u(r,z,t)}{\partial z}\right|_{z=0} = \frac{u(r,1,t) - u(r,-1,t)}{2\Delta z}$$

and

$$\frac{\partial u(r,z,t)}{\partial r} = \frac{u(r+\Delta r,1,t) - u(r-\Delta r,1,t)}{2\Delta r}$$

However, Alterman and Rotenberg (1969) showed that this method becomes progressively more inaccurate after several time steps. They determined that one should use a centered difference for the r derivative, but a backward difference for the z derivative:

$$\left.\frac{\partial u(r,z,t)}{\partial z}\right|_{z=0} = \frac{u(r,1,t) - u(r,0,t)}{\Delta z}$$

and the same for the w component of displacement.

u(r,0,t) and w(r,0,t), the displacements at the ficticious layer, are easily evaluated when the boundary stress condition is applied. For axisymmetric problems it is

$$\text{Pressure} = \tau_{zz} = \lambda\left(\frac{\partial u}{\partial r} + \frac{u}{r} + \frac{\partial w}{\partial z}\right) + 2\mu\frac{\partial w}{\partial z}$$

$$0 = \tau_{rz} = \mu\left(\frac{\partial w}{\partial r} + \frac{\partial u}{\partial z}\right)$$

The difference expression for these conditions are then, with a driving pressure P(M,1,t),

$$P(M,1,t) = \lambda(M,1) \left[\left(\frac{u(M+1,1,t) - u(M-1,1,t)}{2} \right. \right.$$

$$+ \frac{u(M,1,t)}{(M-1)\Delta r} + \frac{w(M,1,t) - w(M,0,t)}{\Delta r}$$

$$+ 2\mu(M,1) \left(\frac{w(M,1,t) - w(M,0,t)}{\Delta r} \right)$$

$$0 = \left(\frac{w(M,1,1,t) - w(M-1,1,t)}{2\Delta r} \right.$$

$$+ \left(\frac{u(M,1,t) - u(M,0,t)}{\Delta r} \right.$$

from which $u(r,0,t)$ and $w(r,0,t)$ can be evaluated and substituted into the expression for

$$\left.\frac{\partial u(r,z,t)}{\partial z}\right|_{z=0}$$

and

$$\left.\frac{\partial w}{\partial z}(r,z,t)\right|_{z=0}$$

which are then used in the homogeneous elastic wave equation for the mesh near the free surface. Thus, in the case of the free surface we treat the boundary condition separately, using the homogeneous equation, whereas the other velocity changes are handled automatically using the heterogeneous equation.

Non-reflecting boundary

Elimination from the observed signal of energy reflected from the boundary introduced into the problem by truncating the medium is accomplished either by placing the boundary sufficiently far from each point of observation, or by devising a non-reflecting boundary. Extending the mesh requires more computer storage and longer run times, which makes this alternative a poor choice.

A non-reflecting boundary in one dimension is easy to create because one knows the relation between the wave striking the boundary and its reflection, and it is therefore possible to cancel the reflected wave at future times near the boundary. This is even possible to do with both P and S waves arriving, since one can work with both transverse and longitudinal displacements. In two and three dimensions this simple approach becomes impossible and only very poor approximate cancelling schemes can be devised in special cases.

Another possible approach would be to introduce damping into the equations. By increasing the damping coefficient while adjusting the elastic parameters (to keep the impedance of the damped and non-damped regions equal) it should be possible to remove all reflections.

The easiest way to introduce damping is by adding $k'\dot{u}$ and $k'\dot{w}$ velocity-dependent terms to the u and w component equations, respectively. This method works fine for a few time steps and then errors start to accumulate, causing the damping to become inefficient and impractical. A more effective way of introducing damping is to treat the elastic parameters as operators and to add a time derivative

$$\lambda \rightarrow \lambda + \lambda'\frac{\partial}{\partial t}, \quad \mu \rightarrow \mu + \mu'\frac{\partial}{\partial t}$$

One sees that in the one-dimensional case this amounts to adding a velocity-dependent term giving the familiar damped response. In the three-dimensional axisymmetric problems this approach would generate very complicated expressions for the damped heterogeneous elastic wave equation but it supposedly leads to stable damping of the wave train.

FINITE ELEMENT METHOD

We can summarize the drawbacks of the finite difference method as follows:

1. The lack of a good procedure for creating a non-reflecting boundary where the mesh is terminated makes it necessary to use a very large mesh (the reflections travel faster than the Rayleigh wave we are interested in) or else to rescale the material zones as time advances.

2. The discontinuities in the atoll problem are two-dimensional, and this situation cannot be handled satisfactorily. Explicit codes are intrisically unstable for this type of problem.

We therefore decided to use the finite element method: the evolution of this approach is described in the Introduction of the report.

Application of the finite element method to dynamic problems is reasonably straightforward. In roughly the same manner as the implicit-explicit finite difference schemes, the static equations are solved at each time step, and the stresses and displacements throughout the whole mesh are then input as initial conditions to the identical static problem at the next time step.

It turns out that there are many annoying procedural problems in creating an efficient program for carrying out the dynamic finite element scheme, the most important of which is contriving to enumerate the vertices in the mesh so that the coefficient matrix -- which must be inverted in the program at each time step -- is a band

matrix of small bandwidth. It is not practical to invert a 1,000 by 1,000 matrix at each of 1,000 time steps, at least until the millenium of ultra-parallel computations arrives.

We made a literature search, using services of DDC, and found a highly sophisticated finite element program -- the SLAM code -- which was developed for the Air Force by the Illinois Institute of Technology (Costantino, 1968). The program documentation consists of five inch-thick volumes, and there was a time delay while our project personnel mastered them. However, the total delay was clearly much less than would have been required to develop an equivalent program from scratch.

Additional difficulties were encountered at this point. When after a nine-month delay following our request a copy of the program arrived, we found that it was an old version written for the CDC 6600 and it was riddled with errors, both elementary FORTRAN errors and logical mistakes. It was clear that what we received was not a working version of the code, and we were unable to obtain a working version despite repeated requests.

Part of the program was written in 6600 assembly language, so the process of correcting the program required day-to-day use of that type of machine. We obtained an in-house terminal to a 6600, and in addition we simultaneously simplified and condensed the code into a version suitable for running test uses on the CDC 1604 which at that time was available in the Seismic Data Laboratory (SDL) computer center.

After study and experimentation, we decided to adopt a generalization of the implicity/explicit scheme used in the SLAM code, the Newmark Beta Method (Newmark, 1959). This scheme has the advantage that it allows the user to control the way the time-step acceleration varies between the time steps. The method is described by three difference equations:

$$M\underset{\sim}{a}_{n+1} + D\underset{\sim}{v}_{n+1} + Kx_{n+1} = \underset{\sim}{f}_{n+1}$$

$$\underset{\sim}{v}_{n+1} = \underset{\sim}{v}_n + \frac{h}{2}(\underset{\sim}{a}_n + \underset{\sim}{a}_{n+1}) \tag{3}$$

$$\underset{\sim}{x}_{n+1} = \underset{\sim}{x}_n + \underset{\sim}{v}_n h + (\frac{1}{2} - \beta)h^2 \underset{\sim}{a}_n + \beta h^2 \underset{\sim}{a}_{n+1}$$

where β is the parameter which controls the variation of acceleration, M is the mass matrix, D the damping matrix, and K the stiffness matrix. In the SLAM code as we received it, $\beta = 0$. This scheme is explicit only

when D = 0, since in that case successive values of displacement and acceleration can be obtained by inverting only the diagonal mass matrix. The scheme is explicit in general if the velocity damping matrix is diagonal.

The first major revision we made to the code was to install the general implicit scheme, which is represented by the "solved" difference equations:

$$(K + Q)\underset{\sim}{x}_{n+1} = \underset{\sim}{f}_{n+1} + Q\underset{\sim}{x}_n + (hQ-D)\underset{\sim}{v}_n$$

$$- [\tfrac{h}{2}D + (\beta-\tfrac{1}{2})h^2Q]\underset{\sim}{a}_n \tag{4}$$

$$\underset{\sim}{a}_{n+1} = \frac{1}{\beta h^2}[\underset{\sim}{x}_{n+1} - \underset{\sim}{x}_h - \underset{\sim}{v}_n h + (\beta-\tfrac{1}{2})h^2\underset{\sim}{a}_n]$$

$$\underset{\sim}{v}_{n+1} = \underset{\sim}{v}_n + \tfrac{h}{2}(\underset{\sim}{a}_n + \underset{\sim}{a}_{n+1})$$

where

$$Q \equiv \frac{1}{\beta h^2}(\tfrac{h}{2}D + M).$$

Numerical solution of these equations involved inverting the augmented stiffness matrix at every time step. This was accomplished through standard inversion techniques; the matrix was initially block upper-triangularized and stored on tape. The back substitution process was then carried out from this tape at every time step (for general discussion of these techniques, see Wilkison, 1965). The storage required for the matrix calculations necessarily reduced the maximum mesh bandwidth from 100 to 45 on a machine with 32K words of core. The same procedure was also programmed for a 360/67, and the advantage in computing speed over the 1604 compensated for the increased number of calculations required at each time step.

At that time, we also considerably streamlined the SLAM program by deleting the option for handling plastic deformation, which is not relevant to our problem.

After the program had been checked out, we proceeded to apply it to elementary problems whose solutions are known analytically.

The simplest of such problems is an end-loaded rod constrained by rollers to have elastic displacement only along its length. The nodes at one end were loaded by a pulse of stress with a duration equal to the time step interval. The node point displacements should thus be step functions beginning at the appropriate elastic wave arrival time. The actual calculations showed oscillations superimposed on the solution. Figure 5 shows the calculation. Replacing the pulse source with a Gaussian

time variation for the source reduces these oscillations (Figure 6). Introducing damping does not decrease the amplitude of the oscillations, but does decrease the sharpness of compression in the wave front, and makes the back side of the step function into a slowly decaying ramp.

Changing the Newmark β-parameter or the integration time interval did not affect the amplitude of the spurious oscillations, but did decrease their period. When the rod thickness was doubled and divided into two parallel rows of elements of half the original thickness, the calculated results were identical to the original rod with a single row of square elements. This implies that slight changes in the small main diagonal frequencies, while maintaining the same time step, do not affect the calculations.

Other test cases involved varying the size of the elements in the direction transverse to the axis of the rod; none of these variations affected the solutions. What did affect the calculations was variation in the size of elements in the direction of the rod axis.

Figure 7 shows the nodal displacements along the rod. The amplitude of the spurious oscillations increases when the wave front reaches the area of the rod where the element lengths change.

The wavefront velocity is within 2% of the theoretical value, which we regard as satisfactory agreement.

We also studied the classical problem of a line

source at the surface of a homogeneous halfspace (Lamb, 1964). The mesh used is shown in Figure 8. For convenience, and without lack of generality for the purpose of studying the agreement between the calculated solution and the theoretically known solution, we assumed a Poisson solid; $o = 1/4$. The time step was 0.4 seconds, and the P wave velocity 1/4 feet/second. The mesh size was chosen such that the P wave travel time across the smallest element in the mesh was equal to the time step. A delta function source was assumed to be applied during the first time step, and removed for all subsequent times. No damping was used.

The output is shown in Figures 9 and in the frequency-wavenumber spectrum (Figure 10). The frequency-wavenumber spectrum was computed from the output along the surface of the halfspace over that portion of the mesh where the spacing of the nodes was uniform, i.e., 0 to 4 feet away from the source node.

The P wave and Rayleigh arrivals are accurately calculated, but the Rayleigh wave is followed by spurious oscillations. The Rayleigh wave has the proper horizontal and vertical amplitudes and polarity, and has retrograde elliptical particle motion.

In checking through possible reasons for the errors, we discovered that the boundary condition at the free surface was not being properly met. Even though the forces at all the nodes at the surface of the mesh were constrained to vanish, the vertical and radially tangential stresses did not vanish.

We therefore decided to constrain the boundary stress through the use of the stress tables already calculated by the program. This was accomplished through a Lagrange multiplier technique. To illustrate it, we first consider the static problem which is solved by minimizing the strain energy:

$$u = \frac{1}{2}\underset{\sim}{x}^T K \underset{\sim}{x} \tag{5}$$

with the stress matrix constraint:

$$S\underset{\sim}{x} = \underset{\sim}{\sigma}_a \tag{6}$$

The solution to the problem posed by equations (5) and (6) is obtained by inserting a vector of Lagrange multipliers, $\underset{\sim}{\lambda}$ and minimizing the modified strain energy:

$$u' = \frac{1}{2}\underset{\sim}{x}^T K \underset{\sim}{x} + (\underset{\sim}{x}^T S^T - \underset{\sim}{\delta}^T)\lambda \tag{7}$$

The minimization of equation (7) gives the solution as:

$$\begin{aligned} \underset{\sim}{\lambda} &= -(SK^{-1}S^T)^{-1}\underset{\sim}{\sigma}_a \\ K\underset{\sim}{x} &= S^T(SK^{-1}S^T)^{-1}\underset{\sim}{\sigma}_a = \underset{\sim}{f}_e \end{aligned} \tag{8}$$

where $\underset{\sim}{f}_e$ is now the effective force.

The dynamic problem proceeds in much the same manner, resulting in the following equations:

$$(K + Q)\underset{\sim}{x}_{n+1} = S^T\underset{\sim}{\lambda}_{n+1} + Q\underset{\sim}{x}_n + (hQ - D)\underset{\sim}{v}_n$$

$$- [\tfrac{h}{2}D + (\beta-\tfrac{1}{2})h^2Q]\underset{\sim}{a}_n \tag{9}$$

$$S\underset{\sim}{x}_{n+1} = \underset{\sim}{\sigma}_{n+1}$$

which can be solved to give:

$$\underset{\sim}{r}_n \equiv Q\underset{\sim}{x}_n + (hQ - D)\underset{\sim}{v}_n - [\tfrac{h}{2}D + (\beta-\tfrac{1}{2})h^2Q]\underset{\sim}{a}_n$$

$$\underset{\sim}{\lambda}_{n+1} = [S(K + Q)^{-1}S^T]^{-1}\underset{\sim}{\sigma}_{M+1} - S(K + Q)^{-1}\underset{\sim}{r}_n \tag{10}$$

$$(K + Q)\underset{\sim}{x}_{n+1} = S^T[S(K + Q)^{-1}S^T]^{-1}\underset{\sim}{\sigma}_{n+1}$$

$$+ \{I - S^T[S(K + Q)^{-1}S^T]^{-1}S(K + Q)^{-1}]\underset{\sim}{r}_n$$

The third version of SLAM solves these equations. The penalty paid is an increase in run time by a factor of two and a decrease in maximum mesh bandwidth from 45 to 29. This version is still capable of being run in a 32K machine. With it, the two stress components τ_{zr} and σ_{zz} are as specified on the constrained surface for all time.

The output from this version of the program is shown in Figures 11 and 12. Figure 11 shows spurious oscillations between the P wave arrival and the Rayleigh wave, in addition to the same "himalayan" effect following the Rayleigh wave seen in Figure 9.

The frequency-wavenumber spectra show that the ringing is due to travelling energy having lower group velocity than the Rayleigh wave, and which is normally dispersed. The result of the dispersion appears to be due to the design of the mesh. There also appears to be wavenumber aliasing in the horizontal direction; this is also unexplained. The displacement at the source node (Figure 13) shows that these effects are not due to ringing at the origin. We therefore believe that this sort of mesh is not capable of accurate representation of the solution, and that more detail in the mesh (possibly around the region of the source) would be necessary to obtain accurate results. However, this refinement is beyond the capability of the computers available to us at the present time.

One of us (DWM) has continued to study this problem, and has made use of Wilson's code (Wilson, 1969). He obtained results similar to those reported here. He has

also modified the original SLAM code by replacing the lumped-mass matrix by a consistent-mass matrix (Zienkiewicz, 1967). The results of this modification are not yet available. The work of Goudreau and Taylor (1972) has provided new insight which may aid in solving this class of elastic wave problems.

REFERENCES

Alterman, Z.S. and Rotenberg, A., 1969, Seismic waves in a quarter plane: Bull. Seism. Soc. Am., v. 59, p. 347-368.

Alterman, Z.S., Aboudi, J. and Karal, F.C., Jr., 1970, Pulse propagation in a laterally heterogeneous solid elastic sphere: Geophys. J. Roy. Ast. Soc., v. 21, p. 243-260.

Costantino, C.J., 1968, Stress waves in layered media: Final Report to Space and Missiles Systems Organization (SAMSO), Norton Air Force Base, California: SAMSO TR 68-181.

Goudreau, G.L. and Taylor, R.L., 1972, Evaluation of numerical integration methods in elasto dynamics: Lawerence Livermore Lab., Report No. UCRL-73854.

Holzer, F., 1966, Calculation of seismic source mechanisms: Proc. Roy. Soc. (London) Math. Phys. Sci., A-290, p. 408-429.

Lamb, H., 1964, On the propagation of tremors over the surface of an elastic solid: Phil. Trans. Roy. Soc. (London), A-203, p. 1-42.

McGarr, A. and Alsop, L.E., 1967, Transmission and Reflection of Rayleigh waves at vertical boundaries, JGR, v. 72, p. 2169-2180.

McGarr, A., 1969, Amplitude variations of Rayleigh waves - propagation across a continental margin: Bull. Seis. Soc. Am., v. 59, p. 1281-1305.

REFERENCES (Cont'd.)

Newmark, N.M., 1959, A method of computation for structural dynamics: J. Engineering Mechanics Division, ASCE, v. 85 Em3, p. 67-94.

Tobey, Robert, Baker, J., Crews, R., Marks T. and Victor, K., 1967, PL/1 FØRMAC Interpreter User's Reference Manual, IBM 360D03.3.004.

Wilkinson, J.H., 1965, The Algebraic Eigenvalue Problem, Clarendon Press, Oxford.

Wilson, Edward L., 1969, Elastic dynamic response of axisymmetric structures report to waterways experiment station: U.S. Army Corps of Engineers: Department of Civil Engineering, University of California, Berkeley, California.

ACKNOWLEDGEMENTS

This research was sponsored by the Advanced Research Projects Agency under Project Vela Hotel, and monitored by the Air Force Office of Scientific Research under contract F-14620-69-C-0082. Grateful acknowledgement for many helpful discussions and suggestions is made to C.J. Constantino, D.G. Harkrider, Z. Alterman, and J. Greene, G. Nickel. Dr. Alterman very generously made available to us her finite-difference computer program.

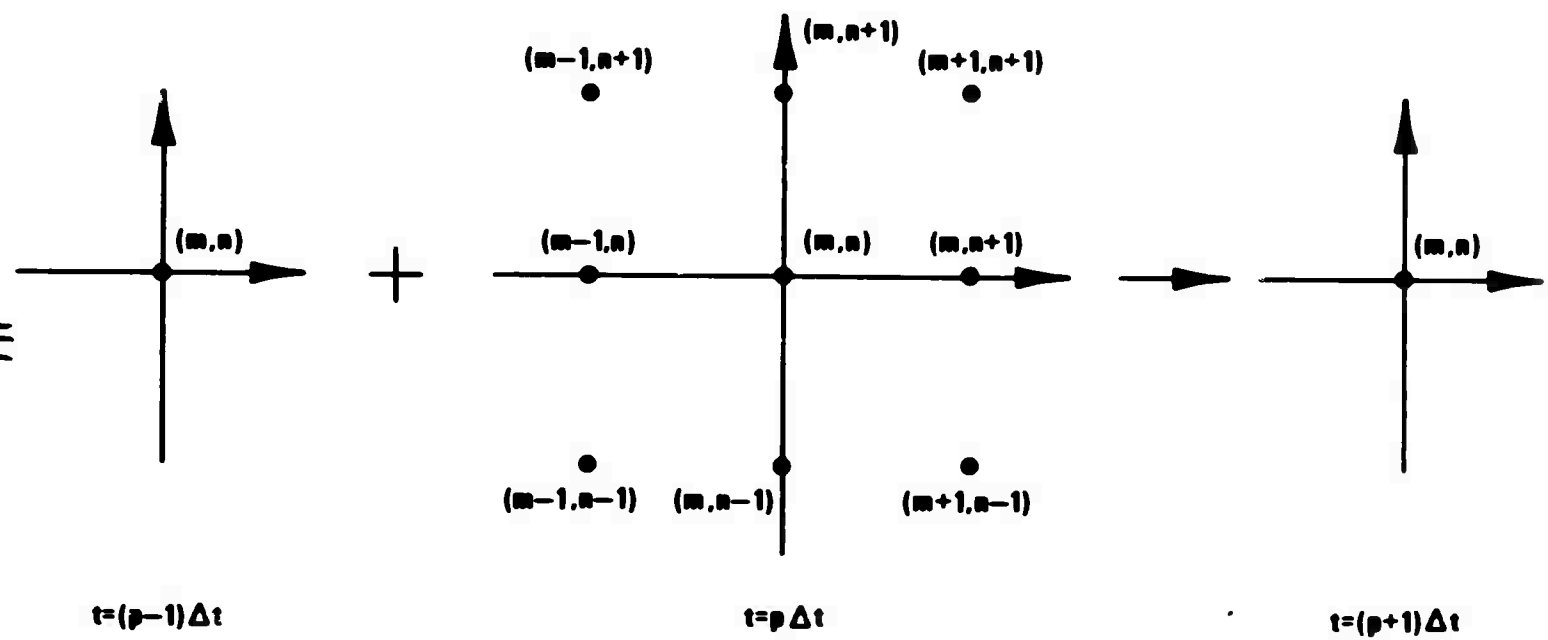

Figure 1. Schematic diagram of the finite difference displacement calculation.

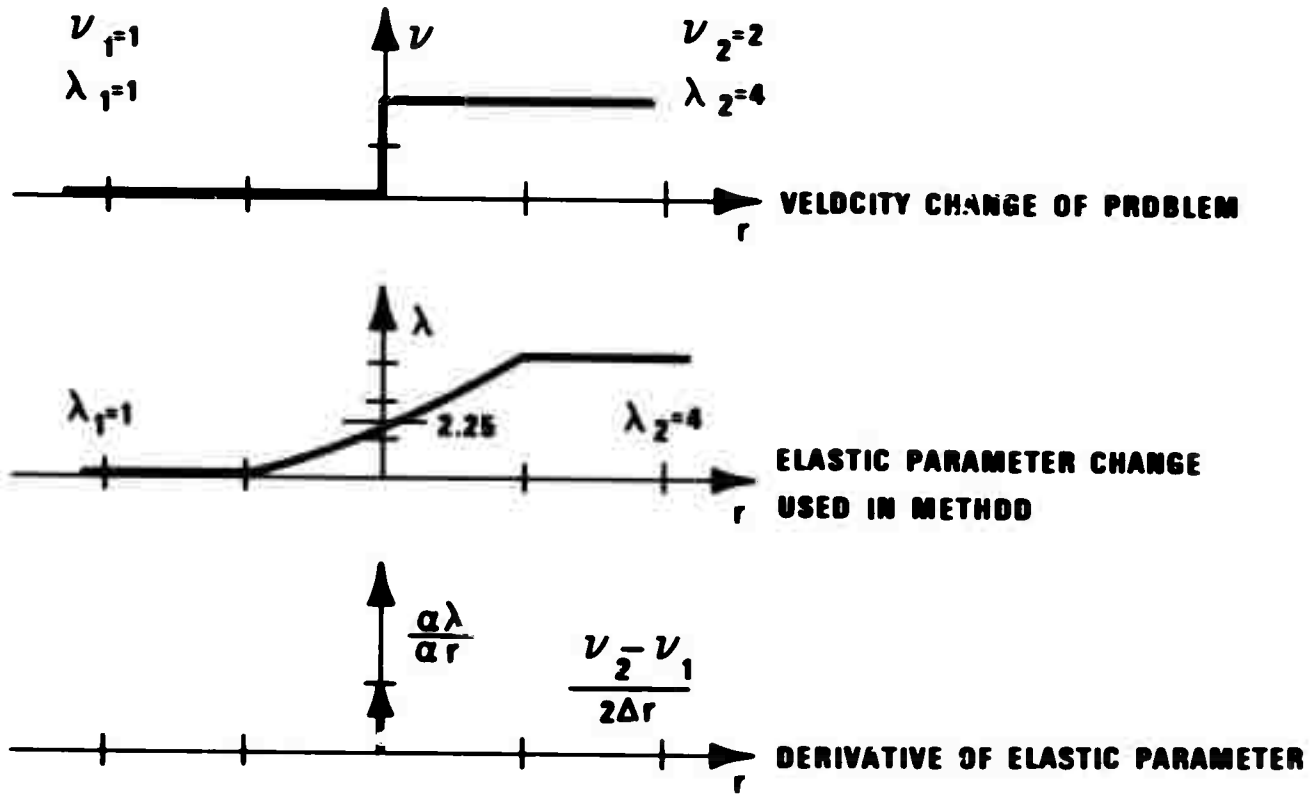

Figure 2. Representation of the derivatives of the elastic parameters at material boundaries for the finite difference method.

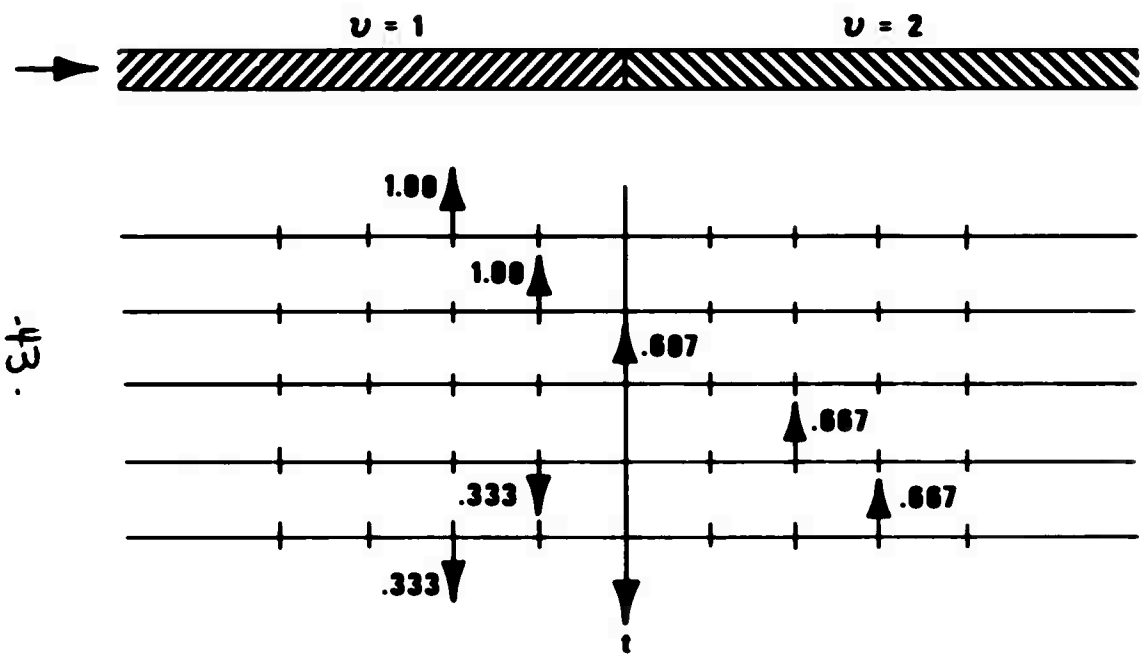

Figure 3. Transmission and reflection of a pulse at a material boundary using the finite difference method.

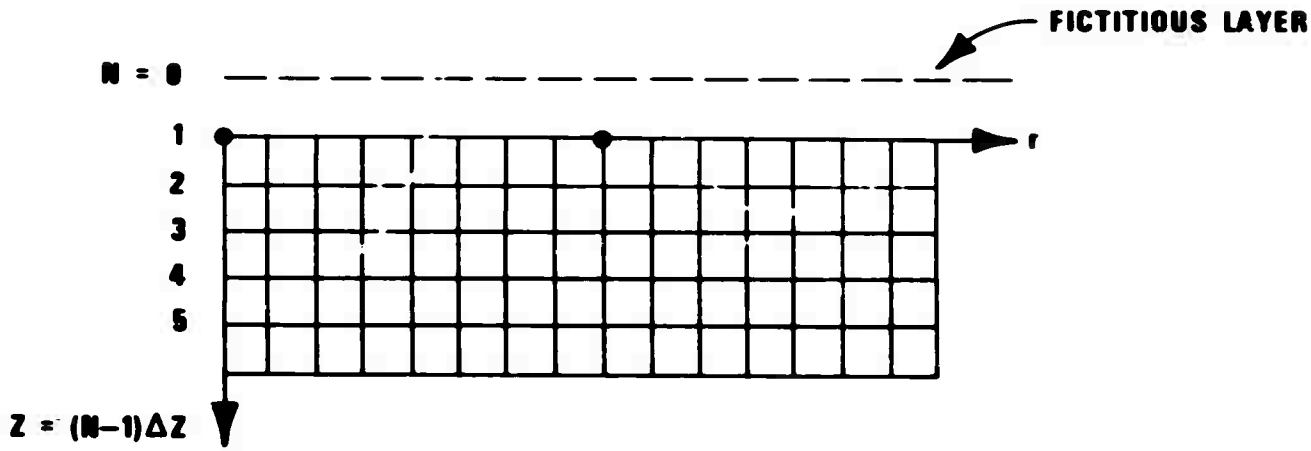

Figure 4. Material mesh which gives satisfactory difference equations at the free surface.

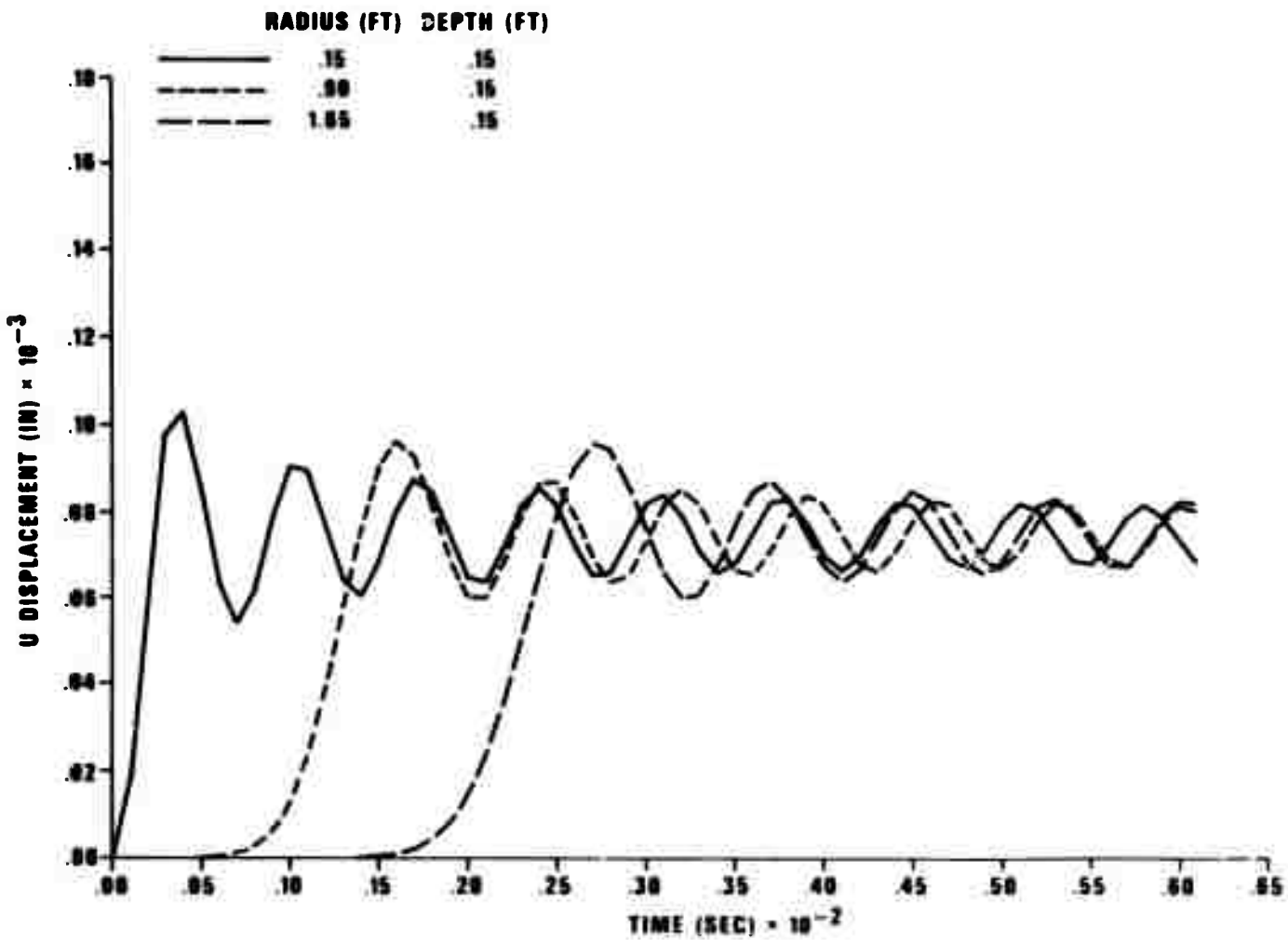

Figure 5. Longitudinal displacement of the "standard" one-dimensional rod with square wave pulse input.

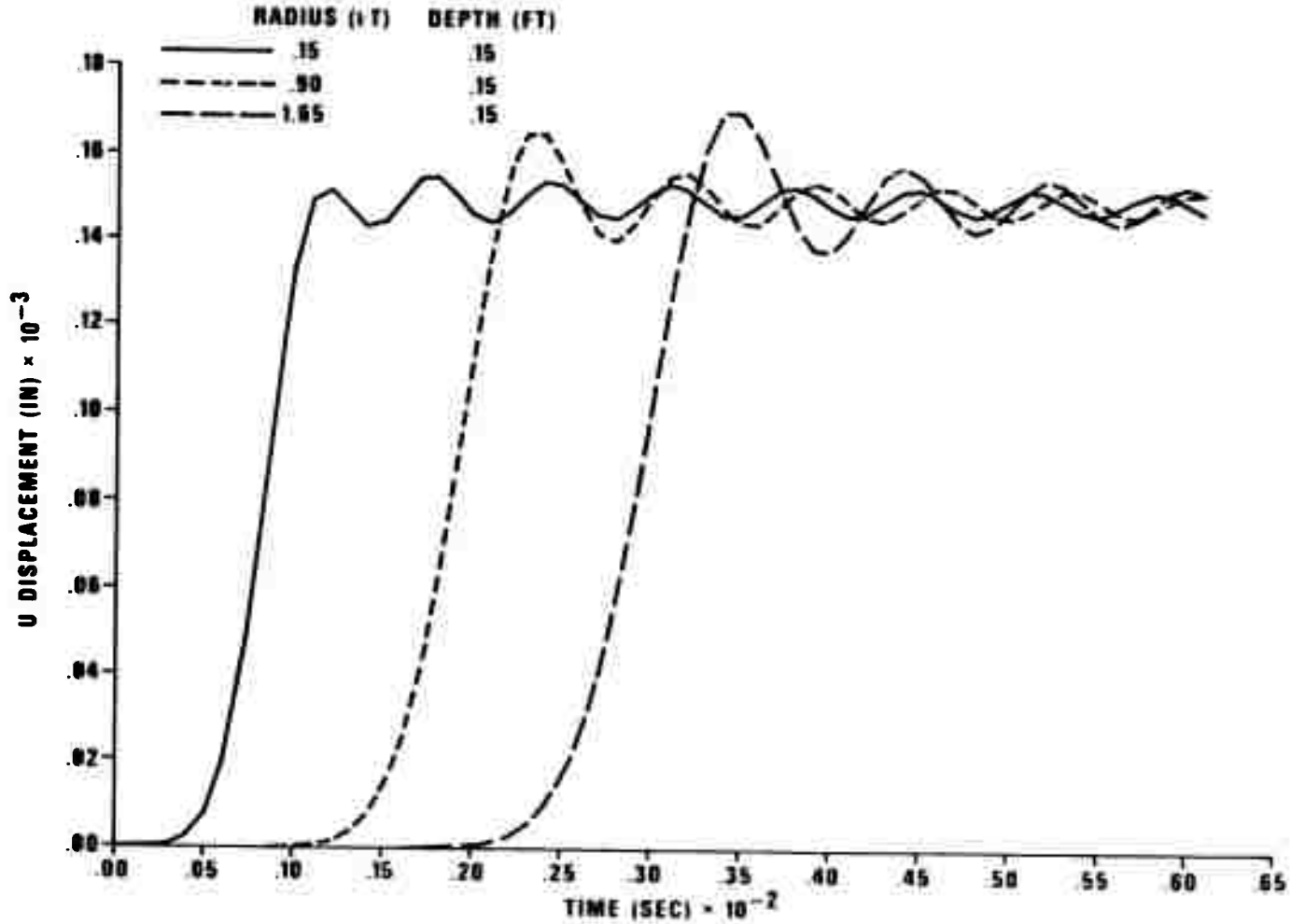

Figure 6. Longitudinal displacement of the "standard" one-dimensional rod with Gaussian shaped pulse input.

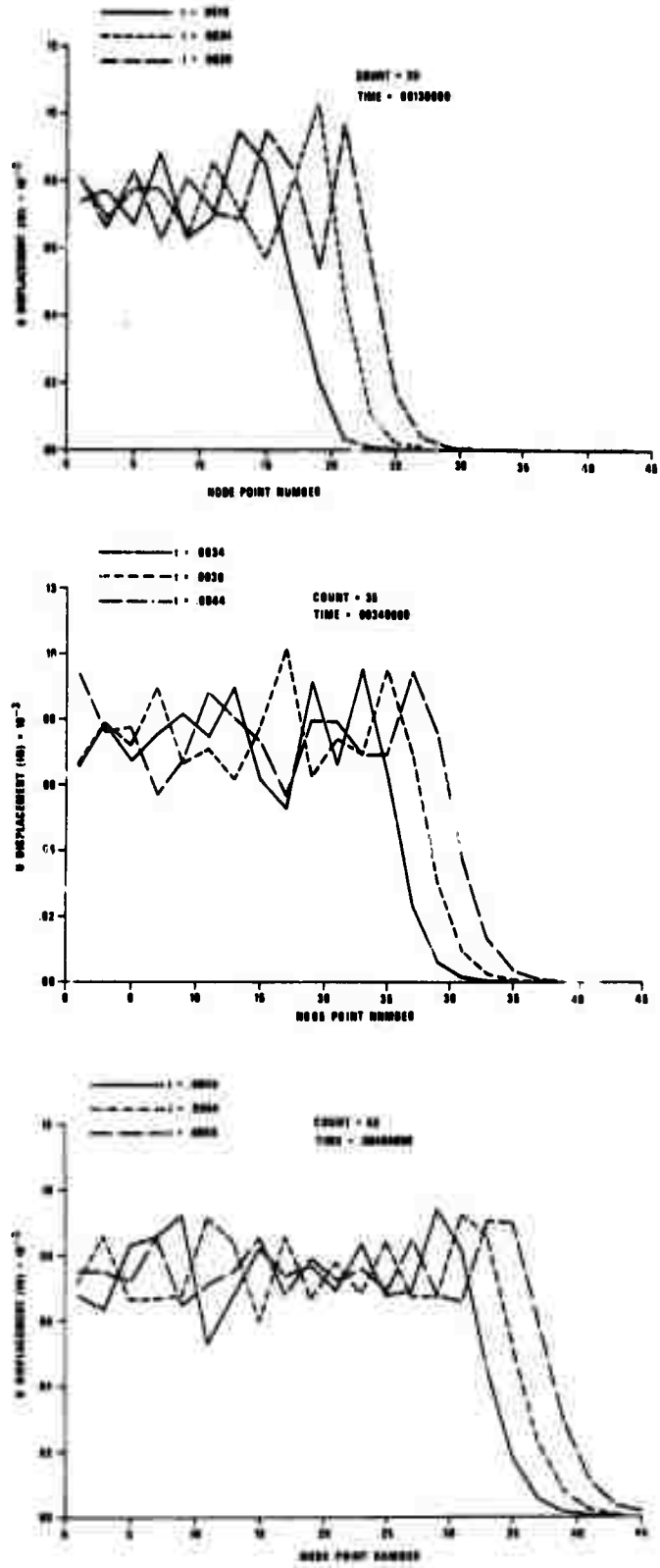

Figure 7. "Snapshots" of longitudinal displacements in a rod where the elements double in length following nodes 19 and 20, at times between 0.0019 and 0.0059 seconds.

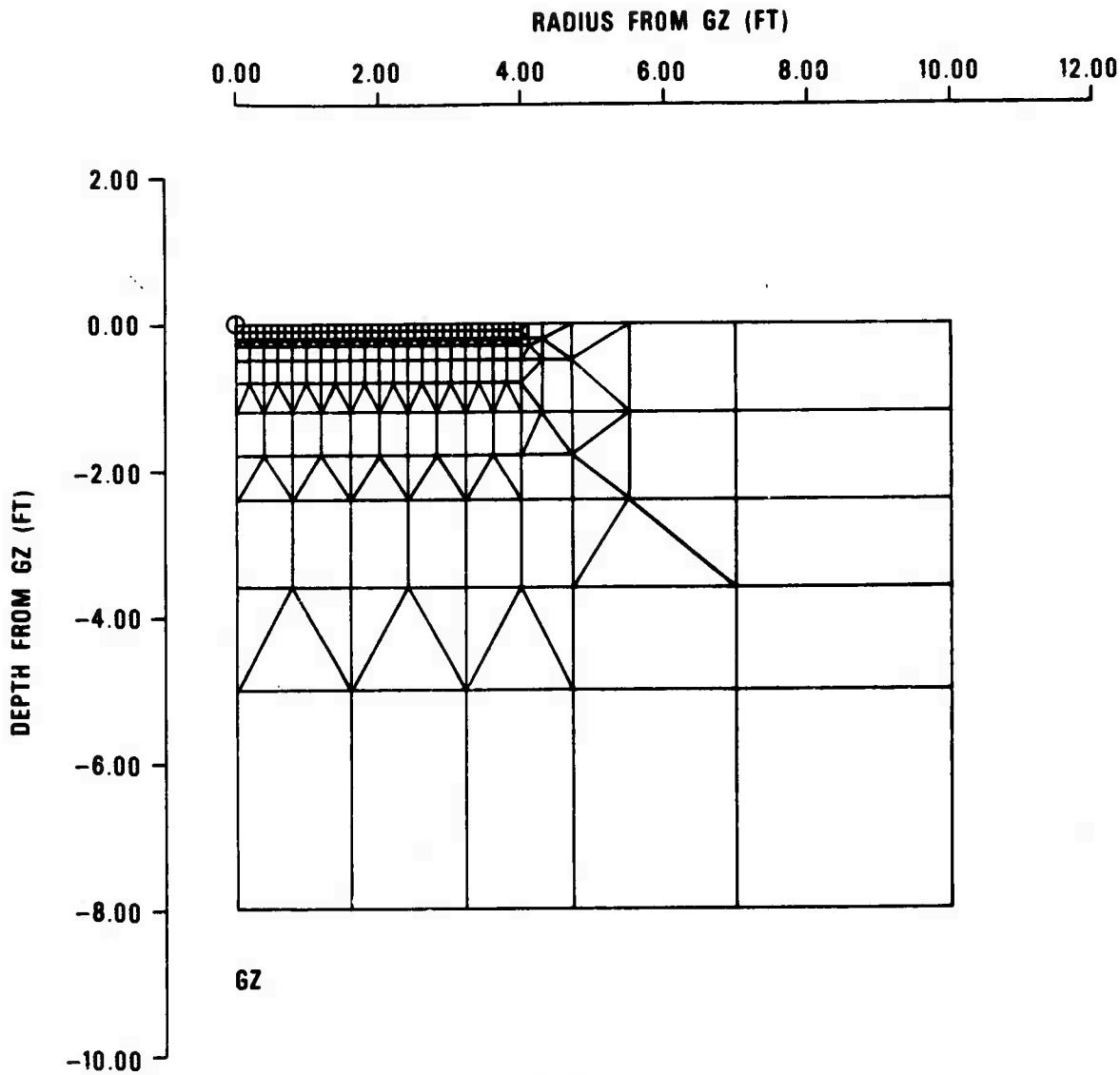

Figure 8. Homogeneous isotropic halfspace mesh used for solving Lamb's problem.

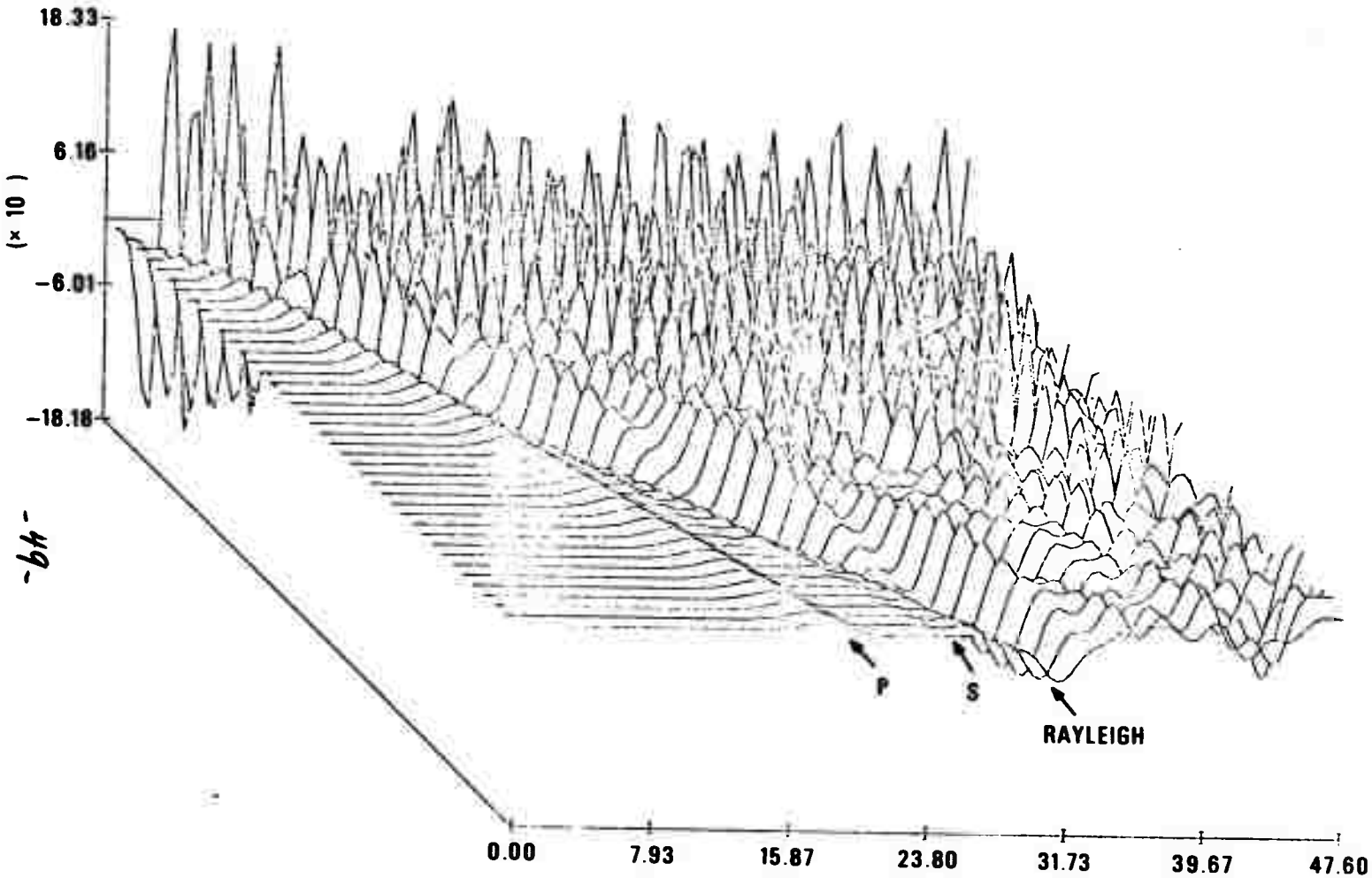

LAMBS PROBLEM WITH MESH 7. BETA=1/4, DT=2/5, D=20

Figure 9a. u displacement for Lamb's problem with unconstrained surface stress.

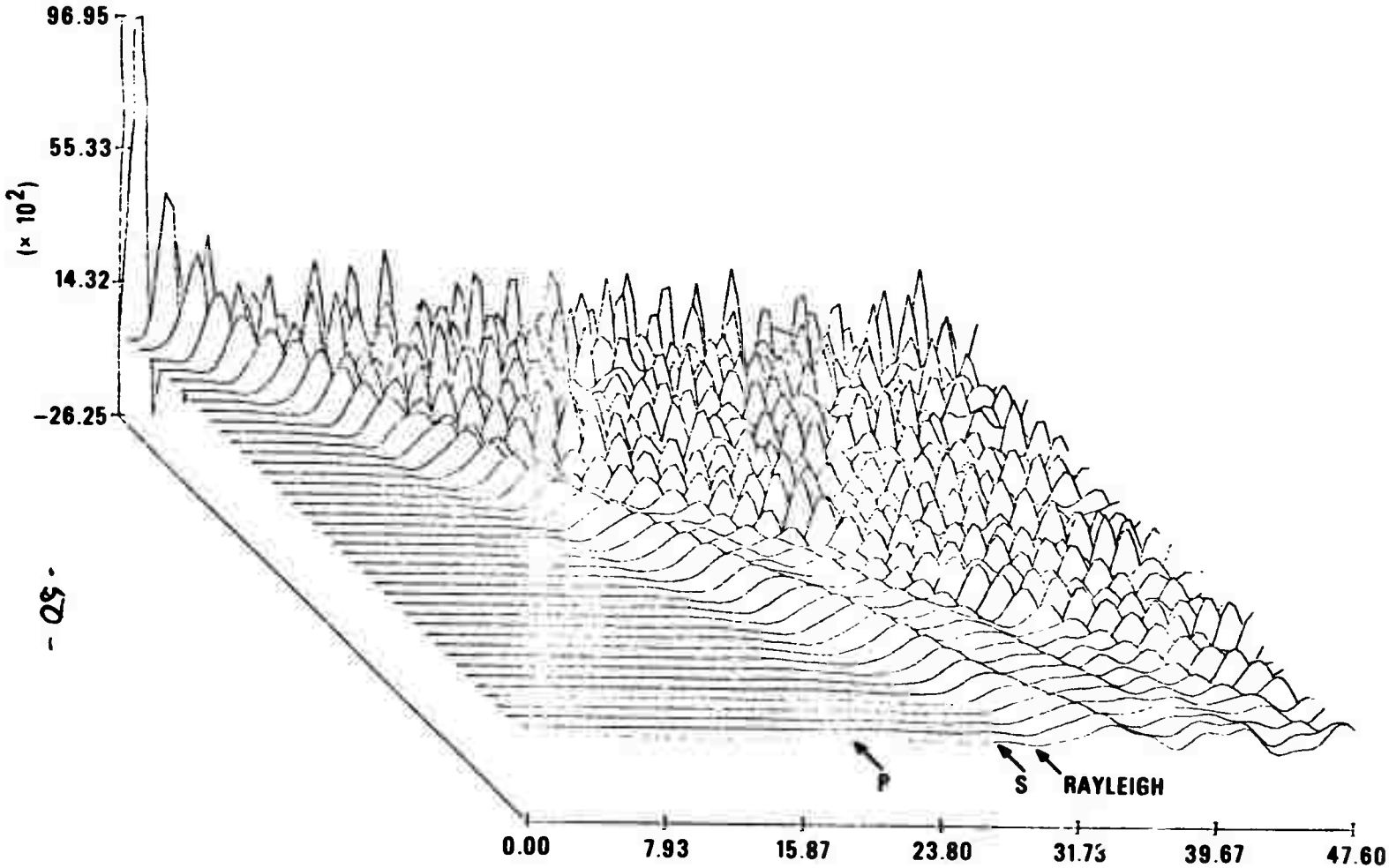

LAMBS PROBLEM WITH MESH 7. BETA=1/4, DT=2/5, D=20

Figure 9b. w displacement for Lamb's problem with unconstrained surface stress.

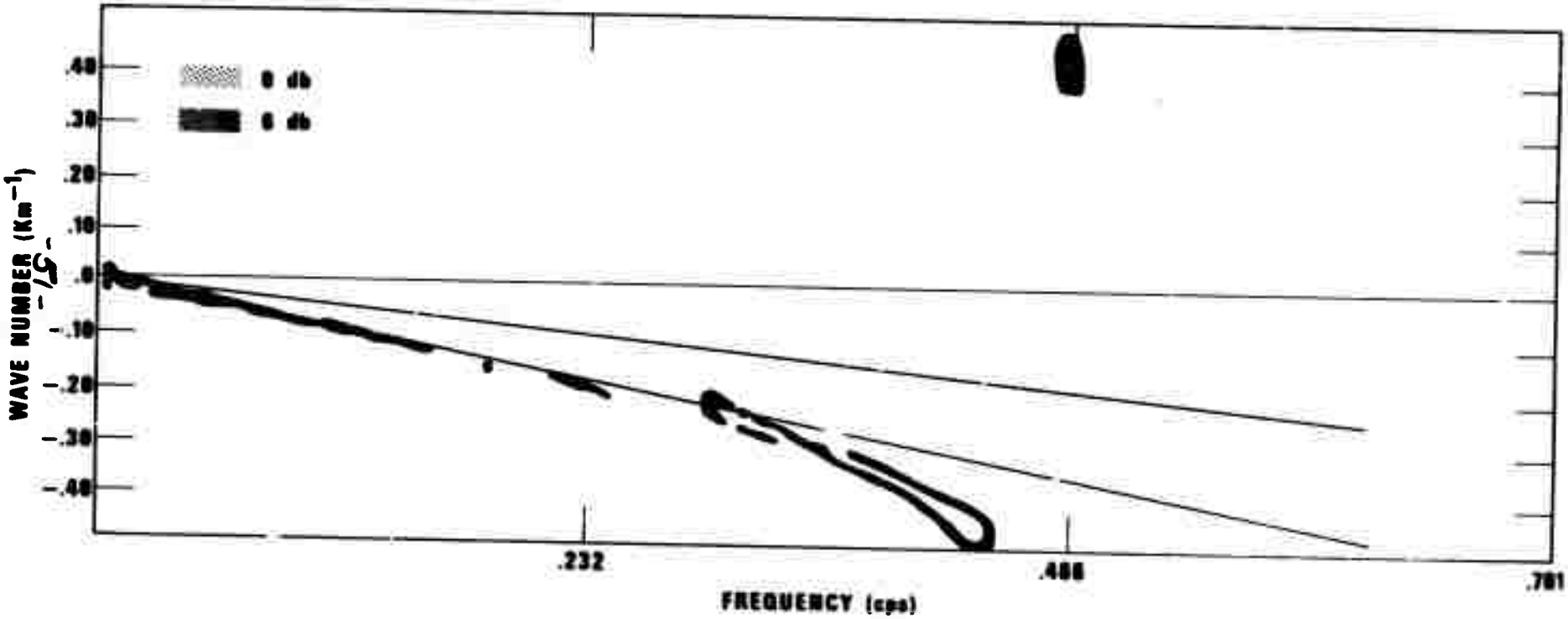

Figure 10. f-k plot of w component for Lamb's problem with unconstrained surface stress. Contour interval is 3 db.

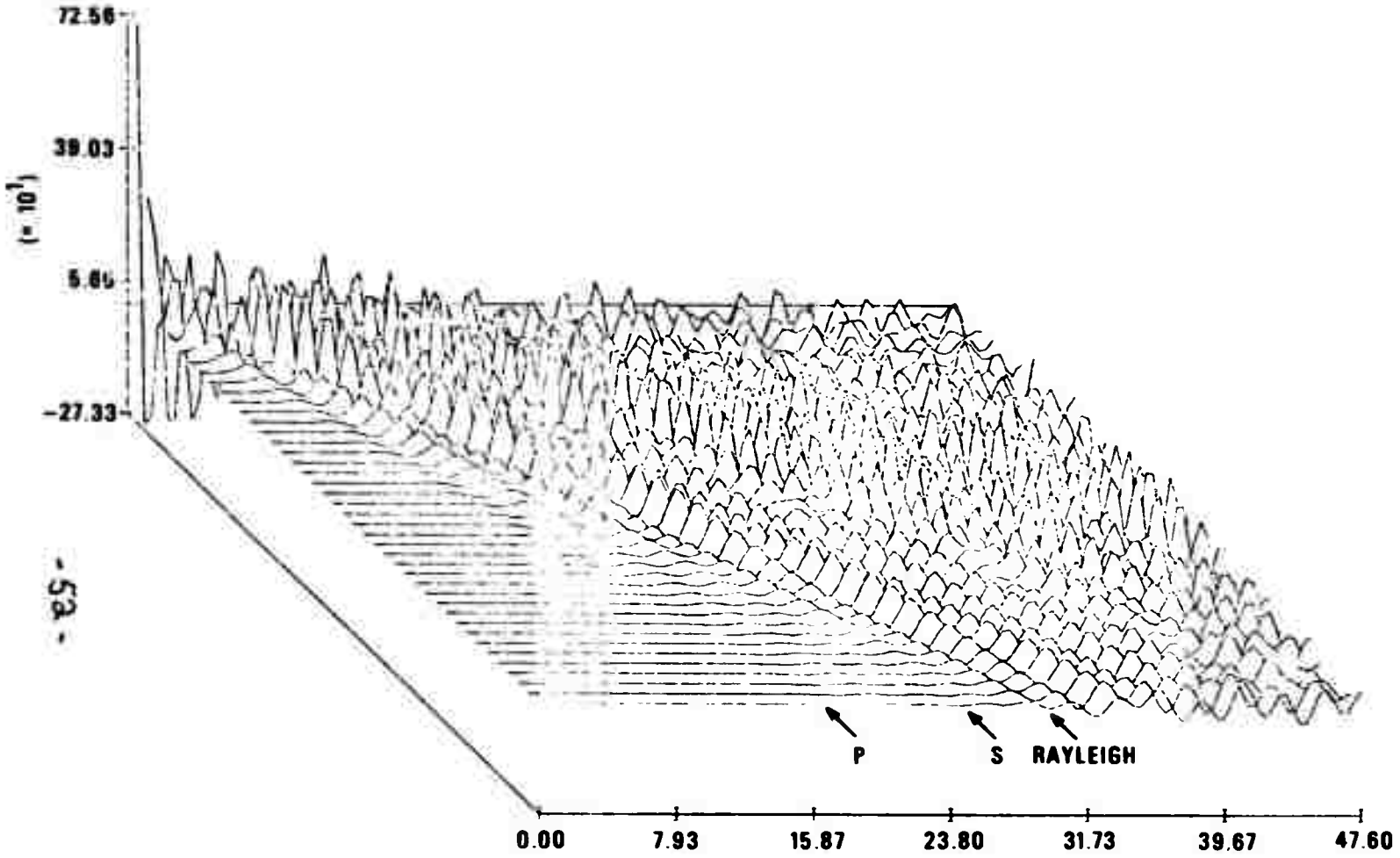

Figure 11a.u displacement for Lamb's problem with constrained surface stress.

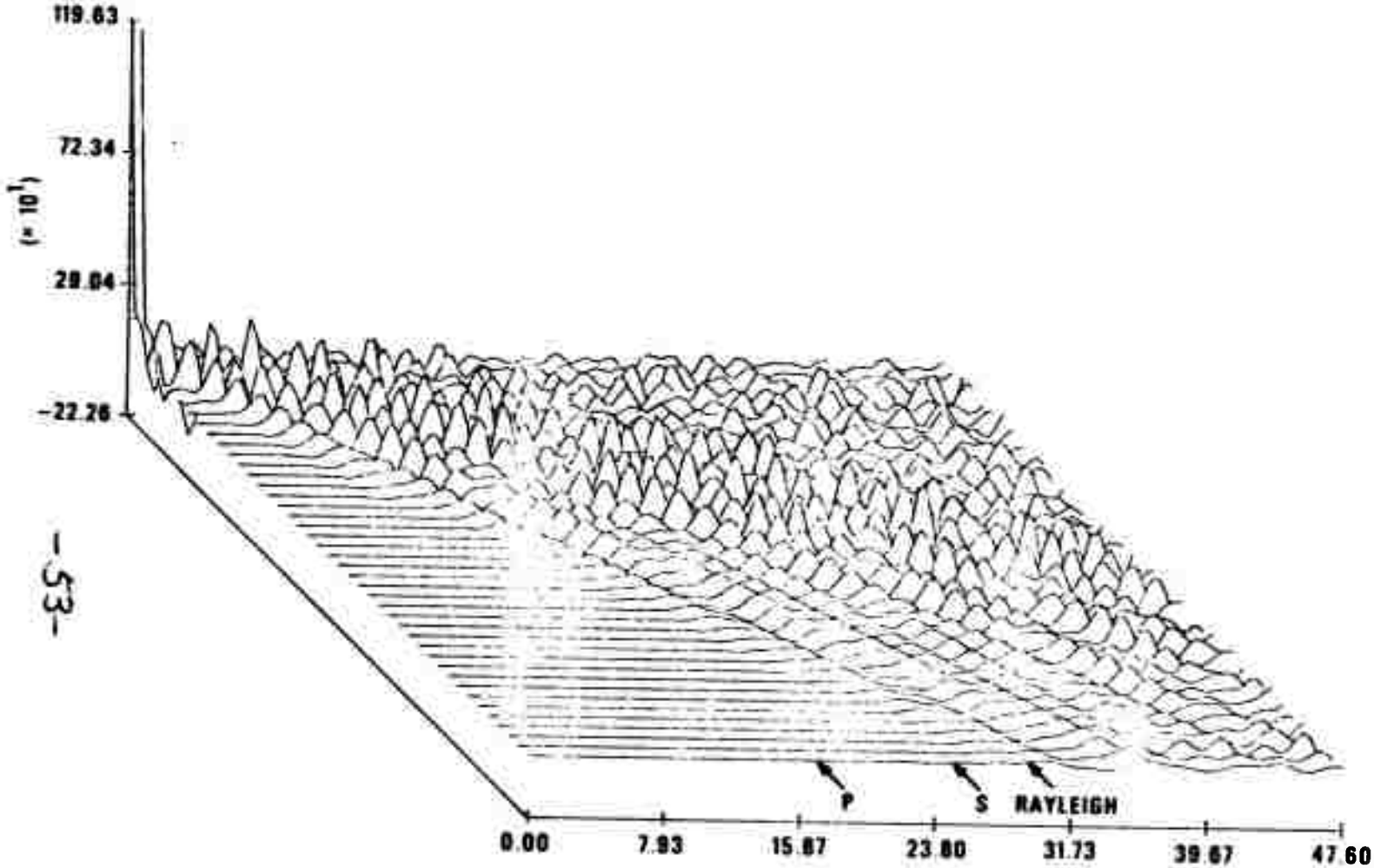

Figure 11b. w displacement for Lamb's problem with constrained surface stress.

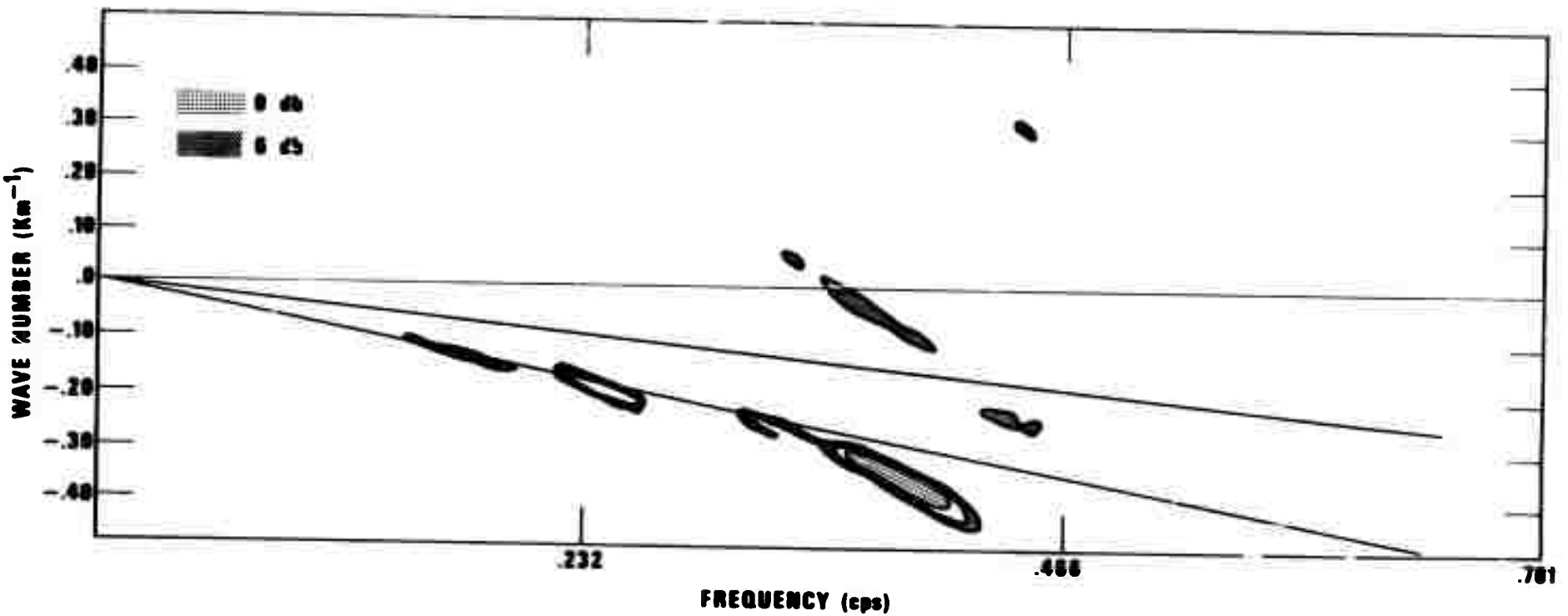

Figure 12. f-k plot of w component for Lamb's problem with constrained surface stress.